SPANDIDOS PUBLICATIONS

Genome-wide expression profiling of urinary bladder implicates desmosomal and cytoskeletal dysregulation in the bladder exstrophy-epispadias complex

LIHONG QI[1,2], KUN CHEN[3], DAVID J. HUR[4], GARIMA YAGNIK[5], YEGAPPAN LAKSHMANAN[6], LORI E. KOTCH[4], GERALD H. ASHRAFI[4], FRANCISCO MARTINEZ-MURILLO[7], JEANNE KOWALSKI[8], CYRILL NAYDENOV[9], LARS WITTLER[10,11], JOHN P. GEARHART[6], MARKUS DRAAKEN[12,13], HEIKO REUTTER[12,14], MICHAEL LUDWIG[15] and SIMEON A. BOYADJIEV[5,6]

[1]Rowe Program in Human Genetics, Departments of [2]Public Health Sciences and [3]Statistics, University of California Davis, 2825 50th Street, Sacramento, CA 95817; [4]McKusick-Nathans Institute of Genetic Medicine, Johns Hopkins University School of Medicine, Baltimore, MD 21205; [5]Section of Genetics, Department of Pediatrics, University of California Davis, Sacramento, CA 95817; [6]Division of Pediatric Urology, The James Buchanan Brady Urological Institute, Johns Hopkins School of Medicine, Departments of [7]Molecular Biology and Genetics, and [8]Oncology, The Sidney Kimmel Comprehensive Cancer Center, Johns Hopkins University School of Medicine, 600 North Wolfe Street, Baltimore, MD 21287, USA; [9]Department of Chemistry and Biochemistry, Medical University, 2 Zdrave Street, Sofia 1431, Bulgaria; [10]Department of Developmental Genetics, Max-Planck-Institute for Molecular Genetics, Ihnestrasse 63-73, D-14195 Berlin; [11]Institute of Medical Genetics, Charite-University Medicine Berlin, Campus Benjamin Franklin, Hindenburgdamm 30, D-12203 Berlin; [12]Institute of Human Genetics, [13]Department of Genomics, Life and Brain Center, [14]Department of Neonatology, Children's Hospital, [15]Department of Clinical Chemistry and Clinical Pharmacology, University of Bonn, Sigmund-Freud-Str. 25, D-53105 Bonn, Germany

Received October 20, 2010; Accepted December 9, 2010

DOI: 10.3892/ijmm.2011.654

Abstract. The bladder exstrophy-epispadias complex (BEEC) represents a spectrum of urological abnormalities where part, or all, of the distal urinary tract fails to close during development, becoming exposed on the outer abdominal wall. While the etiology of BEEC remains unknown, strong evidence exists that genetic factors are implicated. To understand the pathways regulating embryonic bladder development and to identify high-probability BEEC candidate genes, we conducted a genome-wide expression profiling (GWEP) study using normal and exstrophic human urinary bladders and human and mouse embryologic bladder-precursor tissues. We identified 162 genes differentially expressed in both embryonic and postnatal human samples. Pathway analysis of these genes revealed 11 biological networks with top functions related to skeletal and muscular system development, cellular assembly and development, organ morphology, or connective tissue disorders. The two most down-regulated genes desmin (*DES*, fold-change, -74.7) and desmuslin (*DMN*, fold-change, -53.0) are involved in desmosome mediated cell-cell adhesion and cytoskeletal architecture. Intriguingly, the sixth most overexpressed gene was desmoplakin (*DSP*, fold-change, +48.8), the most abundant desmosomal protein. We found 30% of the candidate genes to be directly associated with desmosome structure/function or cytoskeletal assembly, pointing to desmosomal and/or cytoskeletal deregulation as an etiologic factor for BEEC. Further findings indicate that p63, PERP, SYNPO2 and the Wnt pathway may also contribute to BEEC etiology. This study provides the first expression profile of urogenital genes during bladder development and points to the high-probability candidate genes for BEEC.

Correspondence to: Dr Simeon A. Boyadjiev, M.I.N.D. Institute, UC Davis, 2825 50th Street, Sacramento, CA 95817, USA
E-mail: simeon.boyd@ucdmc.ucdavis.edu

Key words: bladder exstrophy, bladder development, cytoskeletal assembly, desmosomal assembly, epispadias, genome-wide expression profiling

Introduction

The bladder exstrophy-epispadias complex (BEEC) represents a rare birth defect thought to be a clinical spectrum ranging from isolated epispadias (EP), to the classic bladder exstrophy (CBE) and to its most severe form, cloacal exstrophy (CE) often referred to as the OEIS (omphalocele, exstrophy of the bladder, imperforate anus, and spinal defects) complex (1-3). Prevalence at birth ranges from 1/30,000 for CBE to

1/200,000 for CE (4). There is a greater proportion of affected males than females, ranging from 1.8:1 to 6:1 (5,6). While the etiology of BEEC remains unknown, strong evidence exists linking its development to genetic effects. The etiological association of genetic determinants is supported by the discrepant male to female ratio (7); a 400-fold increase of the recurrence risk for offsprings of affected individuals (8); observations of rare multiplex families (9); and much higher concordance rates (62% vs. 11%) among monozygotic as compared to dizygotic twins (10). Its non-Mendelian pattern of segregation and the incomplete concordance among MZ twins implies a complex trait model of inheritance.

Typically, the patients with BEEC do not have developmental delays, and with the exception of CE, there are few anomalies outside of the urogenital system (5,6). The associated anomalies observed in BEEC are mesoderm-derived, including omphalocele, hernias, kidney agenesis, imperforate anus, and pelvic dysplasia. This suggests that the genetic insult may be limited to the mesodermal lineage. Indeed, Wood *et al* (11) proposed that BEEC occurred due to the overall deficiency of the somitic and lateral plate mesoderm in the infra-umbilical region. Since this mesodermal cell population forms the muscular components of the bladder and infra-umbilical body wall, it is plausible that a deficiency of this cell population would account for this phenotype.

The emerging picture of BEEC as a complex trait determined by mutations in genes regulating the proliferation and differentiation of the mesoderm and the morphogenesis of the smooth muscle of the urinary bladder motivated the expression studies described in this paper. DNA microarrays have proven to be a powerful technological platform for genome-wide expression profiling (12). This approach has been used successfully for identifying causative genes for various diseases such as craniosynostosis (13), asthma (14-16), heart disease (17-19), and hypospadias (20). To better understand the molecular profile of BEEC and to identify potential candidate genes, we conducted a genome-wide expression profiling study using human urinary bladder at two time-points: human embryonic mesenchyme (EM) surrounding the urogenital sinus at 8 weeks of gestation, and postnatal normal bladders (NB) or exstrophic bladders (EB). To further investigate whether differentially expressed bladder derived genes were expressed in the same relevant organogenesis period in both humans and the mouse, we also studied the gene expression profile of urinary bladders pooled from the same mouse litter at gestational day (GD) 13. The concept behind this study was to identify genes with at least two-fold expression difference between normal and exstrophic bladder smooth muscle that are also expressed in the embryonic period when BEEC occurs. These BEEC candidate genes would be a valid target for further molecular and association studies.

Materials and methods

Tissue collection. This study was approved by the Johns Hopkins Medicine Institutional Review Boards and was conducted in accordance with their guidelines. Prior to sample collection, informed consent was obtained from all individuals or their legal guardians. Mouse tissue samples were obtained under approved animal protection protocol. Upon collection all samples were placed in RNA*later*® tissue collection: RNA stabilization solution (Ambion, Austin, TX) and stored at -80°C until RNA isolation. Procedural steps such as tissue freezing and RNA extraction were performed without time delay between stages.

Prenatal human bladder. Bladder-precursor EM surrounding the urogenital sinus was obtained from 3 human embryos electively aborted by dilatation and curettage (D&C) at 8 weeks of gestation. The dissections were carried out under a dissecting microscope in warm buffered saline solution, with tissue extraction completed within 15 min of termination of the pregnancy. Specimens were then transported in tissue culture media on ice to the laboratory, where 3 primary cultures of the mesenchymal tissue were commenced.

Postnatal human bladder. Three postnatal EB and three postnatal NB (control) tissue samples were collected. EB samples were obtained during surgical repair and consisted of discarded bladder tissue from patients with CBE. Surrounding fat and connective tissue were separated from the smooth muscle. NB samples were obtained during ureter re-implantation and consisted of anonymously collected and de-identified bladder tissue from vesico-ureteral reflux patients who did not have BEEC. Since the bladder size, function and morphology were intact, we assumed these samples to be normal bladder tissue. After removing the inner urothelial and outer serosal layers, the EB and NB specimens were placed immediately in RNA*later* solution (Ambion). In addition, EB and NB samples were race- and gender-matched, with 2 female pairs and 1 male pair. All samples were collected from Caucasian individuals younger than 3 years of age.

Mouse bladder. The urinary bladder and the surrounding mesenchyme were microdissected from C57BL/6 mouse (Charles Rivers Laboratory) embryos at GD13, corresponding to human EM samples. The microdissected target tissues were immediately placed in RNA*later* stabilizing solution, and housed in a -20˚C cold block throughout the dissection period. Only tissues collected within 25 min post-removal of embryos from the uterus were used for RNA isolation to reduce sample degradation. The target tissues from the same litter were pooled together and were transferred to a -80°C freezer for storage until RNA isolation.

RNA isolation, purification, quantification, and quality control. Total RNA was extracted using a standard TRIzol protocol (Invitrogen, Carlsbad, CA) and cleaned up with the RNeasy Micro kit (Qiagen, Valencia, CA). The RNA concentration and integrity were measured and assessed by the RNA 6000 Nano Assay on the 2100 Bioanalyzer (Agilent Technologies, Palo Alto, CA). Prior to target preparation, all samples had verified optimal rRNA 18S:28S ratios of 1:2 and clean run patterns. Post-hybridization analysis of the chip (image analysis and 3'/5' ratios of housekeeping genes) raised no significant concern about the integrity of the starting RNA.

ay preparation, hybridization and data acquisition. s processed using the RNA amplification protocol, as described in the Affymetrix (Santa Clara, CA) expression manual. Briefly, 5 μg of total RNA were used to synthesize first-strand cDNA using oligonucleotide probes with 24 oligo-dT plus T7 promoter as primer (Proligo, Boulder, CO) and the SuperScript Choice System for cDNA Synthesis (Invitrogen). Following double-stranded cDNA synthesis, the product was purified by phenol-chloroform extraction, and biotinylated antisense cRNA was generated through *in vitro* transcription using the BioArray HighYield RNA Transcript Labeling Kit (Enzo Biochem, Farmingdale, NY). Biotinylated cRNA (15 μg) samples were fragmented at 94˚C for 35 min (100 mM TAE, pH 8.2, 500 mM KOAc, 150 mM MgOAc). All human samples were hybridized to the Affymetrix Human Genome U133 Plus 2.0 Arrays, and the mouse GD13 sample was hybridized to the Affymetrix Mouse Genome 430 2.0 Array. For each sample, 10 μg of total fragmented cRNA was hybridized to the microarray for 16 h at 45˚C with constant rotation (60 rpm). The Affymetrix Fluidics Station 450 was used to wash and stain the chips, to remove the non-hybridized target and to stain the biotinylated cRNA by incubation with a streptavidin-phycoerythrin conjugate. The staining was amplified using goat IgG as a blocking reagent, and a biotinylated anti-streptavidin goat antibody, followed by a second staining step with a streptavidin-phycoerythrin conjugate. Fluorescence was detected using an Affymetrix GeneChip Scanner 3000, and image analysis of each GeneChip was done through the Affymetrix GeneChip Operating System Software (GCOS) 1.1.1, using the standard default settings. For comparison between different chips, a global scaling was used, scaling all probe sets to a user-defined target intensity of 150.

Quantitative real-time PCR (qPCR). Reactions for qPCR were performed on an ABI Prism 7900HT Fast real-time PCR system (Applied Biosystems, Foster City, CA, USA) using SYBR-Green for detection. Due to the fact that RNA from the individuals analyzed by expression arrays was not available, the qPCR validation of our results was conducted using bladder tissues from 6 other CBE patients (2 female, 4 males) and 4 controls including 2 tissue samples from healthy males, total bladder RNA (male sample, Ambion) and pooled fetal female bladders RNA harvested between 18 and 23 gestation weeks (Stratagene, TX), respectively. The qPCR was performed for 4 selected genes of interest including 2 down-regulated (*DES*, *DMN*) and 2 up-regulated genes (*AQP3*, *PERP*). Each qPCR assay included 20 ng/ml DNA samples in triplicate. Reaction mixtures (10 μl) contained 0.2 mM of each primer and 5 μl of Power SYBR-Green PCR Master Mix (PE-Applied Biosystems) with cycling conditions as follows: initiation, 50˚C for 2 min; denaturation, 95˚C for 10 min, followed by 40 cycles at 95˚C for 15 sec, and a combined annealing and extension step at 60˚C for 60 sec. The threshold cycles (Ct) values were normalized using the Ct value of 3 reference genes (*BNC1*, *CFTR* and *RNase P subunit p38*) for each DNA sample. Relative quantification was done using the comparative Ct method, also known as the $2^{-\Delta\Delta Ct}$ method (21). Fold-change was defined as $2^{-\Delta\Delta Ct}$, where Ct was the average Ct from 3 replicates, ΔCt =Ct gene of interest -Ct reference gene, and $\Delta\Delta$Ct = ΔCt case - ΔCt control. ΔCt control was calculated by averaging the values from the controls. The sequence of primers used to confirm gene expression alterations in microarray analysis is available upon request.

Data analysis. Raw data were normalized by the Robust Multichip Average (RMA) method. Fold-change analysis was applied to the normalized data to identify transcripts differentially expressed between EB and NB samples. Transcripts were selected based on a minimal change of 2-fold, which has been widely used as a threshold in microarray analysis (22,23). Transcripts with at least 2-fold increase or decrease of expression in EB as compared to NB were further filtered by whether they were expressed in all 3 prenatal human bladders, and they were considered to be expressed if they showed a Present call in the chip analysis from the Affymetrix GCOS in the EM samples. The BEEC candidate gene list consisted of the transcripts that were at least 2-fold overexpressed or underexpressed in common among all 3 pairs of NB/EB samples and were also prenatally expressed.

BEEC candidate genes were categorized into groups based on their functional characteristics using the Onto-Tools (24), an ensemble of web-accessible, ontology-based tools for the functional design and interpretation of high-throughput gene expression experiments through the use of Gene Ontology (GO, http://www.geneontology.org). Ingenuity Pathways analysis (Ingenuity® Systems, http://www.ingenuity.com) was also applied to candidate genes to identify biological networks, based on a comprehensive database representing a large number of individual protein-protein and gene-complex interactions. The software computes a score for each network according to the fit of Focus Molecules using the Fisher's exact test. The score, derived from a P-value from the test, reflects the likelihood of Focus Molecules in a network by chance: a 1 in 100 chance is scored 2, 1 in 1,000 is scored 3, etc. Therefore, scores of ≥2 have ≥99% confidence (and ≥3 have ≥99.9%) of not being generated by random chance alone.

We observed that the genes with the highest degree of differential expression between EB and NB (*DES*, *DMN*, *DSP*) were related to the desmosome, motivating us to investigate whether other candidate genes are also associated with desmosomal function and/or cytoskeletal regulation. Every candidate gene was reviewed in depth and assigned to one of the following 6 categories: 1) significant or known association with desmosome structure/function; 2) lesser known or secondary association with desmosome; 3) association with any cell-cell connectivity function (other types of cell-cell junctions); 4) association with connecting cellular components (e.g., actin, ECM); 5) weak association with any of the above functions; 6) almost certainly no association with the above functions. A gene was defined as an adhesion-related gene if it was assigned to one of the first four categories. For each gene, the following sources were examined and the relevant information was collected: the NCBI Gene database (http://www.ncbi.nlm.nih.gov/sites/entrez?db=gene) that includes functional information, gene ontology and potential interacting genes; the UCSC Genome browser (http://genome.ucsc.edu/) for any pertinent localization information, and the PubMed literature search browser (http://www.ncbi.nlm.nih.gov/pubmed/) to determine any

Table I. Differentially expressed transcripts consistently present in three embryonic mesenchyme samples.

Profile NB vs. EB	Observed	EM1	EM2	EM3	Intersection
Up-regulated	301	148	132	125	102
Down-regulated	283	159	146	123	105
Total	584[a]	307	278	248	207[b]

NB, normal bladder; EB, exstrophic bladder; EM, embryonic mesenchyme; intersection, number of transcripts in common, among all 3 EM samples. [a]584 transcripts correspond to 422 distinct genes; [b]207 transcripts correspond to 162 distinct genes.

previous work that would associate the gene of interest with cell connectivity.

In addition to gene ontology analyses, the expression of candidate genes in midgestation mouse embryos was examined by searching the Molecular Anatomy of the Mouse Embryo Project (MAMEP) database (http://mamep.molgen.mpg.de; Spörle, Werber, Neidhardt, and Herrmann, unpublished data). The MAMEP database represents the largest collection of gene expression data on mouse embryos encountering a broad collection of images of gene expression patterns in mouse embryos at GD9 to GD10, generated by whole mount *in situ* hybridization (25). Therefore, the expression pattern of candidate genes at these developmental stages can be taken as an indication of their functional relevance during early development of the bladder primordium and its associated tissues. To further validate candidate genes, we analyzed their chromosomal localization for physical overlap with regions of putative linkage/linkage disequilibrium identified by our recent work and breakpoints of chromosome rearrangements observed in BEEC patients (7,26,27).

Results

BEEC candidate genes. We analyzed the genome-wide RNA expression profile of 3 race- and gender-matched EB and NB samples. Overall, 54,675 probes representing 47,650 genes were analyzed. Based on fold-change analysis, a total of 584 transcripts, corresponding to 422 distinct genes, showed at least 2-fold difference of expression in all 3 NB/EB samples, including 301 overexpressed and 283 underexpressed transcripts (Table I). Among them, 207 transcripts corresponding to 162 genes were also consistently expressed in all 3 EM samples. These genes formed our BEEC candidate gene list.

Quantitative real-time PCR (qPCR) analysis. To validate the microarray analysis, we performed qPCR for the 2 most underexpressed genes in EB, *DES* and *DMN*, and the 2 overexpressed genes, *AQP3* and *PERP*, using bladder tissues from 6 other CBE patients (2 female, 4 males) and 4 controls. Fig. 1 shows the fold-change in *DES*, *AQP3* and *PERP*. The fold-change values for *DMN* for samples CBE1-CBE4 were too small to be presented graphically. Three out of 4 CBE samples tested for *DES* and 4 out of 4 samples tested for *DMN* showed underexpression as compared with the controls, with fold-change ranging from 0.06-0.65 for *DES* and 0.00004-0.00001 for *DMN*, respectively. Thus, the qPCR confirmed that *DES* and *DMN* were differentially expressed as expected by the microarray analysis. For *AQP3* and *PERP*, not all samples showed the same pattern of expression: 2 out of 4 tested CBE samples were overexpressed, with fold-change values 4.98 and 29.46 for *AQP3* and 2.84 and 3.50 for *PERP*, respectively. The fact that not all tested CBE samples confirmed the expression patterns for *DES*, *AQP3*, and *PERP* may be because the samples used in the qPCR were different from those used for the microarray analysis. Furthermore, as a complex trait, BEEC is likely to be a genetically heterogeneous condition with individuals harboring genetic defects in different, but interacting genes.

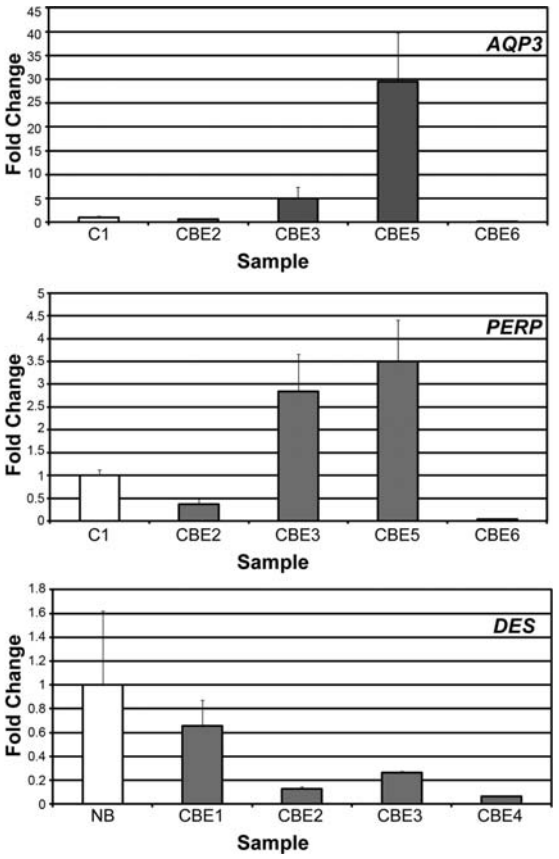

Figure 1. qPCR data of selected genes including one down-regulated (*DES*) and two up-regulated (*PERP*, *AQP3*) genes in microarray analysis. The Y-axis shows the fold-change and the X-axis shows the samples: NB is the average of three controls, C1 represents one control and CBE1-CBE6 are cases. Fold-change < 1 represents down-regulation and fold change > 1 represents up-regulation.

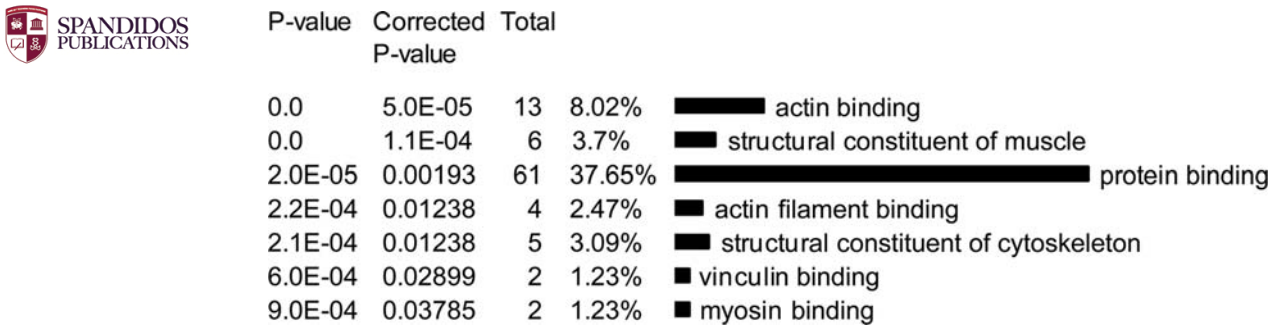

Figure 2. Gene ontology of candidate genes. Frequency distributions according to cellular processes with significant False Discovery Rate (FDR)-corrected P-values. The original P-values and the FDR-corrected P-values are shown in the first and second columns; the number and percentage on the third and fourth columns are the number and percentage of genes that fall within a category.

Gene ontology. Onto-Tools software was used to summarize the cellular processes known to be associated with the 162 genes and those with significant false discovery rate (FDR)-adjusted P-values (<0.05) are shown in Fig. 2. Gene groups include binding of actin, actin filament, myosin and vinculin and structural constituents of muscle and the cytoskeleton, with all groups directly involved in muscle or cytoskeleton formation.

Biological network analyses. Biological network analyses of BEEC candidate genes were performed using the Ingenuity Pathways analysis software. The 162 BEEC candidate genes fell into 11 potential networks, 9 of which included at least 10 candidate genes (Table II). Eight of the 11 networks have top functions related to skeletal and muscular system development and function, cellular assembly and development, tissue development, organ morphology, embryonic development, skeletal and muscular disorders or connective tissue disorders. The largest network consists of 24 candidate genes (including the most underexpressed genes, *DES*, and *DMN*) and has a score of 43, indicating there is almost 100% chance that the network was not randomly generated. The main functions of this network include skeletal and muscular system development and function, tissue morphology, cellular assembly and organization. In particular, 16 of these 24 candidates are located in the cytoplasm (Fig. 3), where the functions for cell expansion, growth and replication are carried out. In the EB samples, 12 (75%) of the 16 genes were underexpressed compared to the NB samples, and these genes are closely involved in muscular system development and function and in tissue morphology.

Genes related to desmosomal function and/or cytoskeletal regulation. The 2 most underexpressed genes in EB, *DES* (fold-change, -74.7) and *DMN* (fold-change, -53.0), encode muscle-specific intermediate filament (IF) proteins, which directly interact with the C-terminal domain of desmoplakin, encoded by the sixth most overexpressed gene in EB samples (*DSP*, fold-change, +48.8). Keratin proteins constitute a major component of the IF in all epithelia, and we observed that 3 type I cytokeratin genes were up-regulated in the EB: *KRT10* (fold-change, +48.7), *KRT18* (fold-change, +8.7) and *KRT19* (fold-change, +28.2).

The observation that the genes with the highest degree of differential expression between EB and NB (*DES*, *DMN*, *DSP*) were related to the desmosome motivated us to investigate whether other candidate genes are also associated with desmosomal function and/or cytoskeletal regulation. By categorizing the 162 BEEC candidate genes, we found that 30.2% (n=49) of them are associated with desmosomal structure/function or with cytoskeletal regulation. Moreover, 34 of the 49 embryologically expressed genes (69.3%) were underexpressed in exstrophic human bladders, implying deficient cytoskeletal organization and more specifically, compromised desmosome-mediated intercellular adhesion in the exstrophic smooth muscle.

Mapping of differentially expressed genes to BEEC candidate loci. To further validate the candidate genes, we analyzed their chromosomal localization for physical overlap with regions of putative linkage/linkage disequilibrium identified by our recent work and breakpoints of chromosome rearrangements observed in BEEC patients. Seven candidate genes, *SLC8A1*, *FLNC*, *CALD1*, *SYNPO2*, *RRM2*, *ROD1*, and *ASS1*, showed partial or complete physical overlap with regions of putative linkage or breakpoints of chromosome rearrangements in BEEC patients (7,26). All these genes were integrated in 5 of our top 10 biological networks: *CALD1* in network 1, *ASS1*, *SLC8A1* and *SYNPO2* in network 2, *RRM2* in network 3, *FLNC* in network 6, and *ASS1* and *ROD1* in network 9 (Table II). *CALD1* encodes caldesmon 1, a calmodulin- and actin-binding protein playing an essential role in the regulation of smooth muscle and cytoskeleton contraction. *RRM2* encodes 1 of 2 non-identical subunits for ribonucleotide reductase and functions downstream of ß-catenin as an inhibitor of Wnt signaling. *SLC8A1* functions as a sodium/calcium exchanger and it rapidly transports Ca^{2+} during excitation-contraction coupling. *SYNPO2* has an actin-binding and actin-bundling activity. *ROD1* may play a role in the regulation of differentiation, and *FLNC* is a muscle-specific filamin playing a central role in muscle cells. It may be involved in re-organizing the actin cytoskeleton in response to signaling events and may also display structural functions at the Z-discs in muscle cells.

Correlation with mouse expression data. A total of 148 mouse orthologous transcripts of these 162 candidate genes were present on the GeneChip Mouse Genome 430 2.0 array, and approximately 80% (n=118) of these mouse orthologs

Table II. Result of Ingenuity pathways analysis based on 162 candidate genes.

	Molecules in network	Score[a]	Focus molecules	Top functions
1	Actin, **ACTN1**, α-Actinin, **CALD1**, CaMKII, **CSRP1**, **DES**, **DSP**, **DTNA**, ERK, **ERMP1**, F Actin, Fascin, **FLNA**, **GEM**, **KLF5,** **LPP**, Mlc, **MYL9** (includes EG:10398), **NEXN**, Pak, **PALLD**, PDGF-AA, **PDLIM1**, **PDLIM7**, **PPIB**, **PPP1R12A**, **PRKACB**, Rock, **S100A11**, **SYNM**, **TNS1**, **TPM1**, **TPM2**, Tropomyosin	43	24	Skeletal and muscular system development and function; tissue morphology; cellular assembly and organization
2	14-3-3, Ap1, **AQP3**, **ASS1**, **BAG2**, **CDCA7**, **CRABP2**, **CTSC**, **DHCR24**, ERK1/2, **FABP5**, **FHL1**, FSH, **GREM1**, **HSPB6**, IgG, IL1, IL12 (complex), Jnk, Mapk, MIR124, P38, MAPK, PDGF BB, **PHLDA2**, Pkc(s), **SC4MOL**, **SFN**, **SLC16A1**, **SLC8A1**, **SOX9**, **SYNPO2**, Tgf ß, **TXNDC17**, **WNT5A**, **ZAK**	39	21	Cell death; cell signaling; embryonic development
3	**ACTC1**, Akt, ALP, **CA12**, Caspase, **CDC2**, Cyclin A, **DTL**, E2f, **EFNB2**, Growth hormone, hCG, **HGF**, Histone h3, Histone h4, Insulin, **KIAA0101**, **KRT10**, **KRT18**, **MCM4**, **MCM5**, Mek, **NUSAP1**, **PCNA**, PP2A, Rb, RNA polymerase II, **RRM2**, **SACS**, Shc, **TOP2A**, **TSPO**, **TYMS**, **UHRF1**, Vegf	33	19	Cancer; DNA replication; recombination and repair; genetic disorder
4	**ALDH1B1**, Calpain, **CD24**, Collagen(s), **DDR1**, FAK, **FERMT2**, Fibrinogen, **FN1**, HSPA1A, IFN ß, **IGFBP2**, **INPP5A**, Integrin, Integrin α2 ß1, Integrin α3 ß1, Integrin α4 ß1, Integrin α, **ITGA2**, **ITGA5**, **ITGA6**, Laminin, MAP2K1/2, NFκB (complex), PI3K, **PRDX4**, Rac, Ras, Ras homolog, **RHOB**, **SLC25A4**, **TFRC**, **TGM2**, **TLN1**, **TXNRD1**	32	18	Cell-to-cell signaling and interaction; cancer; cellular assembly and organization
5	**ACTC1**, AKR1B1, **AMMECR1**, **APRT**, ATP5J2, BAT1, ß-estradiol, **CA12**, **CDCA7**, copper, **CSTB**, **DDX39**, **FAM129A**, FGF1, FOLH1, **GGH**, GJB1, **GJC1**, **GRINL1A**, MIRLET7B (includes EG:406884), MYC, MYO9A, PSMC2, RFC3, RNF115, SARNP, SHMT1, **SHMT2**, SLIT2, **TIMM13**, **TMED3**, TUBG1, UQCRQ, VHL	25	15	Tissue development; organ morphology, amino acid metabolism
6	**CAMK2G**, **CDC42EP3**, **CFL2**, CHD3, CSNK2A2, DKK1, EWSR1, **FLNC**, HDAC1, HNF4A, JUB, JUN, KRR1, MIR297-2, **MLF1IP**, **MREG**, MYOZ2, **NUDT5**, PEX13, **PEX14**, PHB2, Pka, **PLEKHO1**, **PRUNE2**, **PTBP2**, **SGCB**, SGCD, SGCE, SGCG, SNAI2, **SVIL**, **TMEM35**, **TSPAN6**, UMPS, WNT11	25	15	Developmental disorder; skeletal and muscular disorders; tissue development
7	5-hydroxytryptamine, BMP1, CNP, copper, CSNK2A2, ETHE1, FOS, Hd-neuronal intranuclear inclusions, HSP90AB1, HTT, **ITGA2**, **KBTBD10**, **KCNE4**, **KLF5**, LTBP2, MIR17 (includes EG:406952), **MSRB3** (includes EG:253827), MYCN, **NANS**, **PERP**, **RAB27B**, **RNF144B**, RPH3A, RPL12 (includes EG:6136), RPSA, **SCHIP1**, **SLMAP**, STARD13, STRN3, TGFBI, TM4SF1, TMED9, TP53, **TUBA4A**, UNC13D	20	13	Nervous system development and function; neurological disease; cellular development
8	ABLIM1, **AFF3**, **AIM1** (includes EG:202), ARHGDIA, **C6ORF115**, CDH3, CDH5, DSG2, **DSP**, ERBB2, ERBB2IP (includes EG:55914), ETV4, Fascin, FER (includes EG:2241), IRS1, Itgam-Itgb2, ITGAX, ITGB2, **JAM3**, JUP, **KIAA1217**, MUC1, **MYO10**, NCK2, PECAM1, PKN2, RAB8B, RIBC2, **SH3YL1**, SMARCA4, SNAI2, VIM, **ZEB1**, **ZNF185**, **ZWINT** (includes EG:11130)	18	12	Cell-to-cell signaling and interaction; tissue development; cellular movement
9	ACAN, ARFGAP3, **ASS1**, CD3E, **CLIC4**, **CTSC**, DEFB4 (includes EG:1673), DVL1, ESM1, **GPR126**, **GPSN2**, **HN1**, HSPG2 (includes EG:3339), IFNG, MARCKSL1, MGP, MMP10, MUC1, **NDFIP2**, NFAT5, NTF2, PAPPA, PECAM1, PRL, **RAB23**, **ROD1**, SCUBE1, **SCUBE3**, **SEMA3C**, SLC29A1, **SMTN**, SNAI2, SOD1, TNF, TNFAIP2	18	12	Connective tissue disorders; inflammatory disease; skeletal and muscular disorders

Continued.

	Molecules in network	Score[a]	Focus molecules	Top functions
10	ADCY, amino acids, ARAF, Ck2, CSNK2A2, DAPK1, **DMPK**, DUSP7, DYRK1A, geranylgeranyl pyrophosphate, GTP, HTR1B, Importin α/ß, Importin ß, KIF5B, MAP3K8, MC2R, NME2, **NUP50**, PAK3, PKD2 (includes EG:5311), PKN1, PKN2, PPP1R8, **PTPLA**, PTPN2, RANBP2, RNF7, ROCK1, RRAD, **S100A16**, SSB, STIP1, TCOF1, **TGM2**	9	7	Amino acid metabolism; post-translational modification; small molecule; biochemistry
11	**KCTD1**, NFYB	2	1	Cellular development; gene expression

Genes in bold are among the list of 162 differentially expressed candidate genes. [a]The significance score of each pathway is calculated by a hypergeometric test.

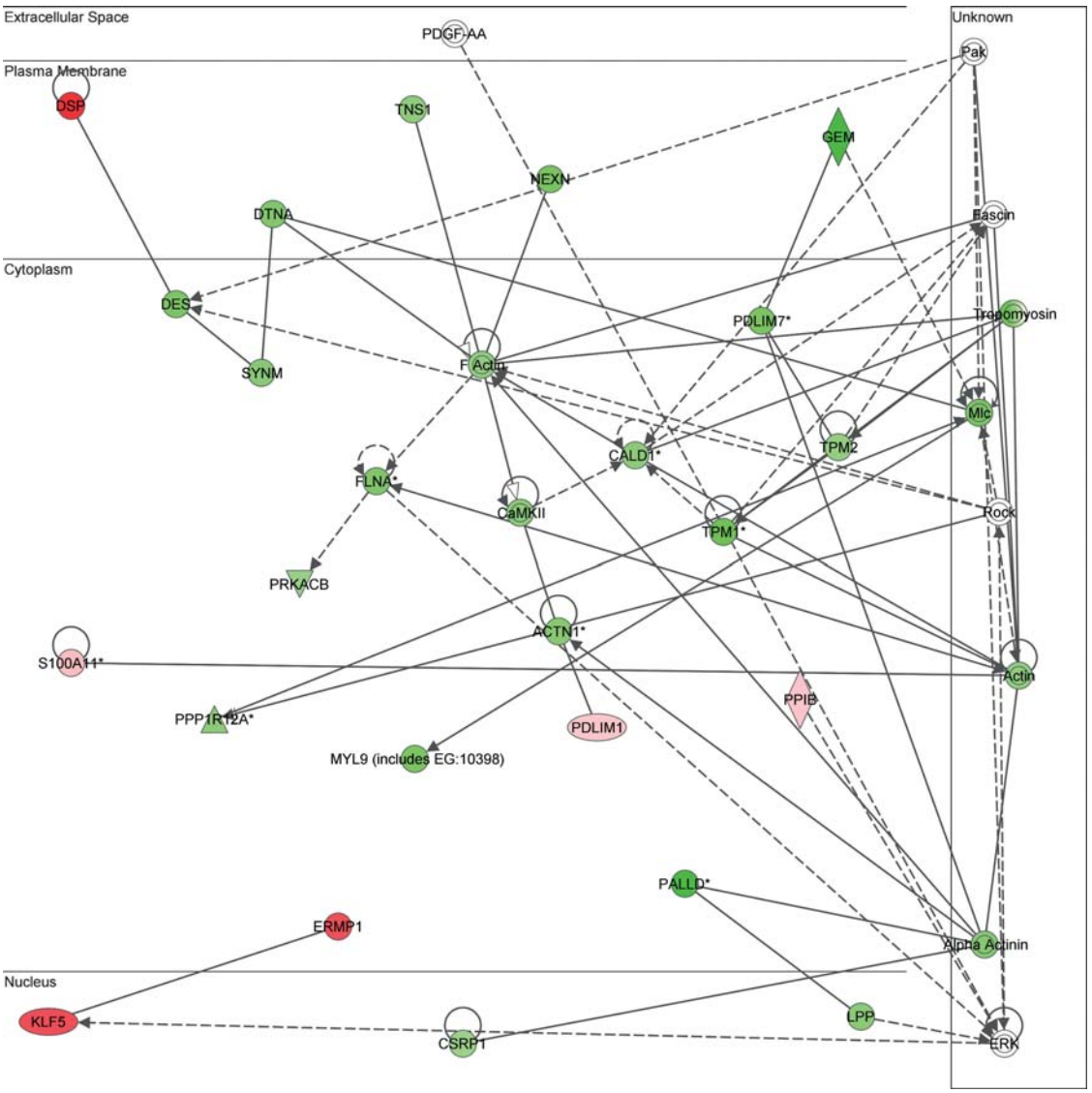

Figure 3. The largest pathway from Ingenuity pathways analysis. A potential network involving 24 candidate genes (filled shapes) according to cellular process. The extent of shading is indicative of the magnitude of regulation. Red and green shadings indicate up-regulation and down-regulation, respectively. The genes shown in transparent circles indicate those from the Ingenuity pathways knowledge base that have been determined as interacting with the list of input candidate genes, on the basis of direct physical, enzymatic, and transcriptional interactions between orthologous mammalian genes from published, peer-reviewed articles. Node shapes indicate function. Diamond designates an enzyme; square, growth factor; triangle, kinase; circle, other; - indicates physical interactions; → indicates functional interaction (activation); | indicates inhibition. Sixteen of the 24 potential candidate genes are present in the cytoplasm.

were expressed at GD13, the time-point corresponding to the human EM. This high degree of concordance is especially significant, since it would be expected that most of the genes that regulate or participate in embryonic bladder development are expressed at the same developmentally relevant period in both humans and the mouse. Moreover, the 118 orthologous genes corresponding to these 148 transcripts were also investigated for their association with desmosomal structure/function or cytoskeletal regulation, and 28.8% (n=34) of these were associated with cell-cell adhesion functions. This percentage is essentially the same as that found in the human data set (30.2%).

Tissue expression pattern of BEEC candidate genes in midgestation mouse embryos. Candidate genes were also examined for their expression in midgestation mouse embryos by search of the MAMEP database. By search of the whole mount *in situ* expression data available in the MAMEP database, 5 of the 87 top ranked up-regulated genes (*PHLDA2*, *WNT5A*, *CRABP2*, *SC4MOL*, *MYO10*) and 11 of the 74 top ranked down-regulated genes (*DES*, *TNS1*, *TPM1*, *CSRP1*, *FN1*, *ACTC1*, *FLNA*, *FLNC*, *LPP*, *CALD1*, *ACTN1*) were found to be expressed in the ventrocaudal mesoderm, the allantoic/umbilical region and/or the hindgut endoderm including the cloacal membrane at GD9-GD10. These tissue expression patterns suggest that these genes are involved in the formation of the infra-umbilical region and additionally confirm the relevance of our microarray results. In particular, the overexpressed gene *PHLDA2* and the underexpressed genes *TPM1*, *CSRP1* and *TNS1* show a strong and defined expression in the ventrolateral area surrounding the cloacal membrane and the basement of the allontois including the bladder primordia. *CALD1* and *ITGA5* expression is more confined to the allantois, while *LPP* and *CRABP2* exhibit expression domains in the area surrounding the hindgut region and cloaca. *FN1* and *WNT5A* transcription takes place in the paraxial and lateral mesoderm in the caudal end of the embryo, the sites of induction and formation of the trunk progenitor tissues. In accordance to their functions in muscle development, *DES* and *FLNC* are expressed in the differentiating somites of the trunk. Additionally, *DES* shows an expression domain in the cloacal membrane and the ureteric cord, while *FLNC* message is detected in the ventrolateral tissues that are associated with the cloaca.

Discussion

BEEC represents a complex group of birth defects caused by failed development of the urogenital system during the first trimester of gestation with a strong evidence for involvement of genetic factors in its etiology. Analyses of genes suggested as candidates by rare chromosomal aberrations, co-occurring syndromes or syndromes with phenotypic overlap, seem rational, but yet have failed to identify causative mutations (5,28-33). Comparative genomic hybridization in a CBE family has only identified a known copy-number variant, most likely unrelated to the phenotype (34) and linkage studies have not identified strong candidate loci (26,27).

We aimed to identify high-probability BEEC candidate genes by expression profiling of normal and exstrophic human urinary bladders, and by focusing on differentially expressed genes present during the relevant bladder embryologic developmental period in humans and the mouse. We identified 422 genes differentially expressed in EB as compared to NB, and among them, 162 were expressed in EM samples, with most of them (73%) also found in mouse embryonic bladder samples corresponding to the human embryonic bladder development period. This finding indicates that most of the genes regulating or participating in embryonic bladder development are expressed in the same relevant period in both human and mouse. In addition, the search of the whole mount *in situ* expression data in the MAMEP database show that 16 candidate genes are expressed in the ventrocaudal mesoderm, the allantoic/umbilical region and/or the hindgut endoderm including the cloacal membrane at GD9-GD10, suggesting that these genes are involved in the formation of the infra-umbilical region, and confirming the relevance of the microarray results. Pathway analysis shows that most of the networks composed of the 162 genes have top functions related to cellular assembly, growth or development, skeletal and muscular system development, organ morphology or connective tissue morphology.

Our analysis of the 162 candidate genes revealed 2 important clues for further studies of BEEC etiology. First, about 30% of candidate genes identified were associated with desmosomal structure/function or cytoskeletal assembly, and 69% of these genes were underexpressed in exstrophic human bladders, suggesting desmosomal and/or cytoskeletal deficiency and/or deregulation. Secondly, *p63*, *PERP*, *SYNPO2* and genes of the Wnt pathway were implicated in BEEC as discussed below.

Desmosomal and/or cytoskeletal deregulation in BEEC. The desmosome, a rivet-like cellular junction structure, is primarily located in epithelial and muscle cells and is specialized for cell-cell adhesion. In addition to maintaining the structural integrity of tissues by resisting shear forces, desmosomes are critical for the formation of organs and tissues during embryogenesis (35). The molecular blueprint of the functional desmosome varies between tissues, but generally consists of 3 principal components including desmosomal cadherins (desmocollins and desmogleins), armadillo type of junctional proteins (plakophilins and placoglobin), and plakin proteins (desmoplakin, plectin, envoplakin and periplakin) (36,37). Plakin proteins serve as an anchor of the IF. As an integral part of the cytoskeleton IF confer resistance to physical stress by distributing mechanical forces throughout a tissue and participate in the formation of supracellular scaffolding that maintains the integrity of tissues. In addition to these classical mechanical functions of the desmosome, there is evidence that mechanical forces transmitted along the length of the IF to the nucleus regulate gene expression (38).

Keratin proteins constitute a major component of the IF in all epithelia and 3 type I cytokeratin genes, *KRT10*, *KRT18* and *KRT19*, were found to be up-regulated in the EB. Even more intriguing was that the 2 most down-regulated genes in EB, *DES* and *DMN* encode muscle-specific IF proteins that directly interact with the C-terminal domain of desmoplakin, encoded by *DSP*, the sixth most overexpressed gene in EB

Evaluation of *DES* in the MAMEP database reveals expressed in the differentiating somites of the trunk, the cloacal membrane and the ureteric cord, in accordance to its function in muscle development. These findings indicate that abnormal formation and/or anchoring of the IF to the desmoplakin component of the desmosome may be the specific cellular defect in BEEC. Our observations warrant morphological analysis of the exstrophic bladder desmosomes by immunofluorescence and electron microscopy.

BEEC candidate genes - p63, PERP, SYNPO2 and genes of the Wnt pathway. Recently, *p63* has been considered as a CBE candidate gene based on a murine knockout model (39,40), however no mutations were found in 15 CBE patients and 5 patients with CE (Ching BJ, *et al*, ASHG Annual Meeting, 478, 2007). We observed that PERP, a tetraspan protein that is a direct p63 downstream target, was 22.2-fold overexpressed in all three human bladder sets and present in all EM samples. Intriguingly, PERP, specifically localizes to the desmosomes where it extends through the plasma membrane to link neighboring cells. Whole-mount *in situ* hybridization studies have demonstrated prominent *PERP* expression in the bladder (41). Furthermore, we have observed overexpression of some transcription-activating p63 isoforms in extrophic bladders and underexpression or complete lack of other ΔN-p63 isoforms, supporting possible desmosomal defects in BEEC (42).

Another highly up-regulated gene was *WNT5A* (14-fold overexpression). During chick cloacal formation, in the mesoderm of the cloacal region, overexpression of the constitutively active form of mouse Gli2 has been reported to induce expression of *WNT5A*, *Ptch1*, *Gli2*, *bmp-4*, and *hoxd-13*, previously shown to play a role in hindgut patterning. Interestingly, *p63* expression in the cloacal endoderm is also up-regulated by Gli2 (43), suggesting that both *WNT5A* and *p63* are regulated by a common upstream pathway. *WNT5A* is strongly expressed in the paraxial and lateral mesoderm in the caudal end of the embryo, and is essential in the caudal extension of the body axis as well as the formation of the external genitalia (44). *WNT5A* has been integrated in network 2 in this study (Table II) and an independent expression profiling of exstrophic bladders has also detected many components of the Wnt pathway (22). Further support for a causal interplay of *WNT5A* in the expression of BEEC, arises from the physical overlap of the *RRM2* gene with a region of suggestive linkage (LOD=1.45 in a dominant model with 80% penetrance) from our own previous work (26). *RRM2*, found to be up-regulated in the EB tissues, functions downstream of ß-catenin as an inhibitor of Wnt signaling (45).

SYNPO2, encoding myopodin or synaptopodin 2 and found to be integrated in network 2 (Table II), is a dual compartment protein displaying actin-bundling activity. It redistributes between the nucleus and the cytoplasm in a differentiation-dependent and stress-induced manner (46). In bladder cancer, previous studies showed differential nuclear localization of myopodin among bladder cancer cells while sharing structural cytoplasmic expression patterns (47). During myotube differentiation, SYNPO2 binds to stress fibers in a punctuated pattern before incorporation in the Z-disc. Vertebrate Z-discs are remarkably complex structures serving several important functions, e.g. stabilizing and anchoring actin filaments during contraction and providing an attachment for other cytoskeletal proteins, such as desmin, nebulin, and titin. It appears that Z-discs of both skeletal and cardiac muscle respond dynamically to mechanical stress through transitions in their lattice structure (48). In this context, *FLNC* and *CALD1*, both down-regulated in the EB tissues, physically overlap regions of putative linkage (26,27), and both encode proteins needed for the stability of the cytoskeleton (49). The function of *CALD1* is also critical for the assembly of the desmosome (50). Moreover, according to the MAMEP database, *FLNC* and *CALD1* show strong expression in the differentiating somites of the allantois at GD9 and GD10, respectively. In light of the increased risk for adenocarcinomas of the exstrophic bladder (51), our observations warrant further investigations of *p53*, *WNT5A* and *SYNPO2* in bladder carcinomas of BEEC patients.

Validation of microarray data. qPCR has been widely used to corroborate microarray expression data. Logically, we attempted to validate our observations by qPCR. However, lack of sufficient RNA from the samples used for the original hybridization experiments forced us to use other exstrophic and control specimens for the qPCR. We found a strong correlation between microarray expression and qPCR data for the two most underexpressed genes, *DMN* and *DES*, and for the most overexpressed gene, *AQP3*. We also documented that another overexpressed integral desmosomal component, *PERP*, a direct p63 downstream target is overexpressed by qPCR in 2 of the 4 tested exstrophic samples (Fig. 1). Due to the limited number and quantity of available exstrophic bladder specimens we could not perform qPCR for more genes. Despite this shortcoming, the consistency of the microarray results, among 3 sets of EB/NB samples corroborated by qPCR analysis strongly support the derived candidate gene list as a valid target for further molecular studies. We believe that our data unequivocally implicate desmosomal and/or cytoskeletal deregulation in the etiology of BEEC and the existing p63-/- mouse model is in agreement with our conclusions, as evident by the p63/PERP (i.e. desmosomal) interactions.

In summary, this study provides the first in depth expression signature of BEEC and has identified a set of candidate urogenital genes expressed during the relevant developmental window of bladder development. The resulting set of 162 genes clearly shows over-representation of genes related to desmosomal and cytoskeletal assembly and comprises a reasonable initial set for future candidate gene studies. In addition, genome-wide association studies (GWAS) and profiling of gene expression are two major technological breakthroughs that allow hypothesis-free identification of candidate genes. Thus the current gene expression study provides a powerful basis for future GWAS or candidate gene association studies on human BEEC to identify relevant genetic contributors.

Acknowledgements

SAB is partially supported by the Children's Miracle Network (CMN) endowed chair in pediatric genetics. This project has

been partially supported through grant M01-RR00052 from the NCRR/NIH, and by a CMN grant CMNSB06 to SAB. LW, MD, ML and HR are members of the 'Network for Systematic Investigation of the Molecular Causes, Clinical Implications and Psychosocial Outcome of Congenital Uro-Rectal Malformations (CURE-Net)' supported by a research grant (01GM08107) from the German Federal Ministry of Education and Research (Bundesministerium für Bildung und Forschung, BMBF).

References

1. Carey JC, Greenbaum B and Hall BD: The OEIS complex (omphalocele, exstrophy, imperforate anus, spinal defects). Birth Defects Orig Artic Ser 14: 253-263, 1978.
2. Gearhart JP: Exstrophy, epispadias, and other bladder anomalies. In: Campbell's Urology. 8th edition. Walsh PC, Retik AB, Vaughan ED and Wein AJ (eds). W.B. Saunders Co., Philadelphia, pp2136-2196, 2002.
3. Martinez-Frias ML, Bermejo E, Rodriguez-Pinilla E and Frias JL: Exstrophy of the cloaca and exstrophy of the bladder: two different expressions of a primary developmental field defect. Am J Med Genet 99: 261-269, 2001.
4. Ebert AK, Reutter H, Ludwig M and Rösch WH: The exstrophy-epispadias complex. Orphanet J Rare Dis 4: 23, 2009.
5. Boyadjiev SA, Dodson JL, Radford CL, Ashrafi GH, Beaty TH, Mathews RI, Broman KW and Gearhart JP: Clinical and molecular characterization of the bladder exstrophy-epispadias complex: analysis of 232 families. BJU Int 94: 1337-1343, 2004.
6. Ives E, Coffey R and Carter CO: A family study of bladder exstrophy. J Med Genet 17: 139-141, 1980.
7. Ludwig M, Ching B, Reutter H and Boyadjiev SA: Bladder exstrophy-epispadias complex. Birth Defects Res A Clin Mol Teratol 85: 509-522, 2009.
8. Shapiro E, Lepor H and Jeffs RD: The inheritance of the exstrophy-epispadias complex. J Urol 132: 308-310, 1984.
9. Reutter H, Shapiro E and Gruen JR: Seven new cases of familial isolated bladder exstrophy and epispadias complex (BEEC) and review of the literature. Am J Med Genet A 120A: 215-221, 2003.
10. Reutter H, Qi L, Gearhart JP, Boemers T, Ebert AK, Rösch W, Ludwig M and Boyadjev SA: Concordance analyses of twins with bladder exstrophy-epispadias complex suggest genetic etiology. Am J Med Genet A 143A: 2751-2756, 2007.
11. Wood HM, Trock BJ and Gearhart JP: In vitro fertilization and the cloacal-bladder exstrophy-epispadias complex: is there an association? J Urol 169: 1512-1515, 2003.
12. Schena M, Heller RA, Theriault TP, Konrad K, Lachenmeier E and Davis RW: Microarrays: biotechnology's discovery platform for functional genomics. Trends Biotechnol 16: 301-306, 1998.
13. Ting K, Vastardis H, Mulliken JB, Soo C, Tieu A, Do H, Kwong E, Bertolami CN, Kawamoto H, Kuroda S and Longaker MT: Human NELL-1 expressed in unilateral coronal synostosis. J Bone Miner Res 14: 80-89, 1999.
14. Erle DJ and Yang YH: Asthma investigators begin to reap the fruits of genomics. Genome Biol 4: 232, 2003.
15. Rolph MS, Sisavanh M, Liu SM and Mackay CR: Clues to asthma pathogenesis from microarray expression studies. Pharmacol Ther 109: 284-294, 2006.
16. Syed F, Panettieri RA, Jr., Tliba O, Huang C, Li K, Bracht M, Amegadzie B, Griswold D, Li L and Amrani Y: The effect of IL-13 and IL-13R130Q, a naturally occurring IL-13 polymorphism, on the gene expression of human airway smooth muscle cells. Respir Res 6: 9, 2005.
17. Heymans S, Schroen B, Vermeersch P, Milting H, Gao F, Kassner A, Gillijns H, Herijgers P, Flameng W, Carmeliet P, Van de Werf F, Pino YM and Janssens S: Increased cardiac expression of tissue inhibitor of metalloproteinase-1 and tissue inhibitor of metalloproteinase-2 is related to cardiac fibrosis and dysfunction in the chronic pressure-overloaded human heart. Circulation 112: 1136-1144, 2005.
18. Li T, Chen YH, Liu TJ, Jia J, Hampson S, Shan YX, Kibler D and Wang PH: Using DNA microarray to identify Sp1 as a transcriptional regulatory element of insulin-like growth factor 1 in cardiac muscle cells. Circ Res 93: 1202-1209, 2003.
19. Ohki R, Yamamoto K, Ueno S, Mano H, Misawa Y, Fuse K, Ikeda U and Shimada K: Gene expression profiling of human atrial myocardium with atrial fibrillation by DNA microarray analysis. Int J Cardiol 102: 233-238, 2005.
20. Willingham E and Baskin LS: Candidate genes and their response to environmental agents in the etiology of hypospadias. Nat Clin Pract Urol 4: 270-279, 2007.
21 Livak KJ and Schmittgen TD: Analysis of relative gene expression data using real-time quantitative PCR and the 2(-Delta Delta C(T)) method. Methods 25: 402-408, 2001.
22. Hipp J, Andersson KE, Kwon TG, Kwak EK, Yoo J and Atala A: Microarray analysis of exstrophic human bladder smooth muscle. BJU Int 101: 100-105, 2008.
23. Okada H, Tajima A, Shichiri K, Tanaka A, Tanaka K and Inoue I: Genome-wide expression of azoospermia testes demonstrates a specific profile and implicates ART3 in genetic susceptibility. PLoS Genet 4: e26, 2008.
24. Khatri P, Bhavsar P, Bawa G and Draghici S: Onto-Tools: an ensemble of web-accessible, ontology-based tools for the functional design and interpretation of high-throughput gene expression experiments. Nucleic Acids Res 32: W449-W456, 2004.
25. Neidhardt L, Gasca S, Wertz K, Obermayr F, Worpenberg S, Lehrach H and Herrmann BG: Large-scale screen for genes controlling mammalian embryogenesis, using high-throughput gene expression analysis in mouse embryos. Mech Dev 98: 77-94, 2000.
26. Ludwig M, Rüschendorf F, Saar K, Hübner N, Siekmann L, Boyadjiev SA and Reutter H: Genome-wide linkage scan for bladder exstrophy-epispadias complex. Birth Defects Res A Clin Mol Teratol 85: 174-178, 2009.
27. Reutter H, Rüschendorf F, Mattheisen M, Draaken M, Bartels E, Hübner N, Hoffmann P, Payabvash S, Saar K, Nöthen MM, Kajbafzadeh AM and Ludwig M: Evidence for linkage of the bladder exstrophy-epispadias complex on chromosome 4q31.21-22 and 19q13.33-41 from a consanguineous Iranian family. Birth Defects Res A Clin Mol Teratol 88: 757-761, 2010.
28. Boyadjiev SA, South ST, Radford CL, Patel A, Zhang G, Hur DJ, Thomas GH, Gearhart JP and Stetten G: A reciprocal translocation 46,XY,t(8;9)(p11.2;q13) in a bladder exstrophy patient disrupts *CNTNAP3* and presents evidence of a pericentromeric duplication on chromosome 9. Genomics 85: 622-629, 2005.
29. Krüger V, Khoshvaghti M, Reutter H, Vogt H, Boemers TM and Ludwig M: Investigation of *FGF10* as a candidate gene in patients with anorectal malformations and exstrophy of the cloaca. Pediatr Surg Int 24: 893-897, 2008.
30. Reutter H, Thauvin-Robinet C, Boemers TM, Rösch WH and Ludwig M: Bladder exstrophy-epispadias complex: investigation of suppressor of variegation, enhancer of zeste and trithorax (*SET*) as a candidate gene in a large cohort of patients. Scand J Urol Nephrol 40: 221-224, 2006.
31. Thauvin-Robinet C, Faivre L, Cusin V, Van Kien PK, Callier P, Parker KL, Fellous M, Borgnon J, Gounot E, Huet F, Sapin E and Mugneret F: Cloacal exstrophy in an infant with 9q34.1-qter deletion resulting from a de novo unbalanced translocation between chromosome 9q and Yq. Am J Med Genet A 126A: 303-307, 2004.
32. Utsch B, DiFeo A, Kujat A, Karle S, Schuster V, Lenk H, Jacobs U, Müller M, Dötsch J, Rascher W, Reutter H, Martignetti JA, Ludwig M and Tröbs RB: Bladder exstrophy and Epstein type congenital macrothrombocytopenia: evidence for a common cause? Am J Med Genet A 140: 2251-2253, 2006.
33. Draaken M, Proske J, Schramm C, Wittler L, Bartels E, Nöthen MM, Reutter H and Ludwig M: Embryonic expression of the cysteine rich protein 61 gene (*CYR61*), a candidate for the development of human epispadias. Birth Defects Res A Clin Mol Teratol 88: 546-550, 2010.
34. Reutter H, Hoischen A, Ludwig M, Stein R, Radlwimmer B, Engels H, Wolffenbüttel K and Weber RG: Genome-wide analysis for micro-aberrations in familial exstrophy of the bladder using array-based comparative genome hybridization. BJU Int 100: 646-650, 2007.
35. Vleminckx K and Kemler R: Cadherins and tissue formation: integrating adhesion and signaling. Bioessays 21: 211-220, 1999.
36. Getsios S, Huen AC and Green KJ: Working out the strength and flexibility of desmosomes. Nat Rev Mol Cell Biol 5: 271-281, 2004.
37. Huber O: Structure and function of desmosomal proteins and their role in development and disease. Cell Mol Life Sci 60: 1872-1890, 2003.

KJ and Simpson CL: Desmosomes: new perspectives on ic. J Invest Dermatol 127: 2499-2515, 2007.
39. Cheng W, Jacobs WB, Zhang JJR, Moro A, Park JH, Kushida M, Qiu W, Mills AA and Kim PCW: Delta Np63 plays an anti-apoptotic role in ventral bladder development. Development 133: 4783-4792, 2006.
40. Ince TA, Cviko AP, Quade BJ, Yang A, McKeon FD, Mutter GL and Crum CP: *p63* coordinates anogenital modeling and epithelial cell differentiation in the developing female urogenital tract. Am J Pathol 161: 1111-1117, 2002.
41. Ihrie RA, Marques MR, Nguyen BT, Horner JS, Papazoglu C, Bronson RT, Mills AA and Attardi LD: *Perp* is a p63-regulated gene essential for epithelial integrity. Cell 120: 843-856, 2005.
42. Ching B, Wittler L, Proske J, Yagnik G, Qi L, Draaken M, Reutter H, Gearhart JP, Ludwig M and Boyadjiev SA: p63 (TP73L) a key player in embryonic urogenital development with significant dysregulation in human bladder exstrophy tissue. Int J Mol Med 26: 861-867, 2010.
43. Liu G, Moro A, Zhang JJ, Cheng W, Qiu W and Kim PC: The role of Shh transcription activator Gli2 in chick cloacal development. Dev Biol 303: 448-460, 2007.
44. Yamaguchi TP, Bradley A, McMahon AP and Jones S: A Wnt5a pathway underlies outgrowth of multiple structures in the vertebrate embryo. Development 126: 1211-1223, 1999.
45. Tang LY, Deng N, Wang LS, Dai J, Wang ZL, Jiang XS, Li SJ, Li L, Sheng QH, Wu DQ, Li L and Zeng R: Quantitative phosphoproteome profiling of Wnt3a-mediated signaling network: indicating the involvement of ribonucleoside-diphosphate reductase M2 subunit phosphorylation at residue serine 20 in canonical Wnt signal transduction. Mol Cell Proteomics 6: 1952-1967, 2007.
46. Weins A, Schwarz K, Faul C, Barisoni L, Linke WA and Mundel P: Differentiation- and stress-dependent nuclear cytoplasmic redistribution of myopodin, a novel actin-bundling protein. J Cell Biol 155: 393-404, 2001.
47. Sanchez-Carbayo M, Schwarz K, Charytonowicz E, Cordon-Cardo C and Mundel P: Tumor suppressor role for myopodin in bladder cancer: loss of nuclear expression of myopodin is cell-cycle dependent and predicts clinical outcome. Oncogene 22: 5298-5305, 2003.
48. Goldstein MA, Michael LH, Schroeter JP and Sass RL: Two structural states of Z-bands in cardiac muscle. Am J Physiol 256: H552-H559, 1989.
49. Gontier Y, Taivainen A, Fontao L, Sonnenberg A, van der Flier A, Carpen O, Faulkner G and Borradori L: The Z-disc proteins myotilin and FATZ-1 interact with each other and are connected to the sarcolemma via muscle-specific filamins. J Cell Sci 118: 3739-3749, 2005.
50. Huber PA: Caldesmon. Int J Biochem Cell Biol 29: 1047-1051, 1997.
51. Husmann DA and Rathbun SR: Long-term follow up of enteric bladder augmentations: the risk for malignancy. J Pediatr Urol 4: 381-385, 2008.